

# JAAS

Accepted Manuscript



This is an *Accepted Manuscript*, which has been through the Royal Society of Chemistry peer review process and has been accepted for publication.

*Accepted Manuscripts* are published online shortly after acceptance, before technical editing, formatting and proof reading. Using this free service, authors can make their results available to the community, in citable form, before we publish the edited article. We will replace this *Accepted Manuscript* with the edited and formatted *Advance Article* as soon as it is available.

You can find more information about *Accepted Manuscripts* in the [Information for Authors](#).

Please note that technical editing may introduce minor changes to the text and/or graphics, which may alter content. The journal's standard [Terms & Conditions](#) and the [Ethical guidelines](#) still apply. In no event shall the Royal Society of Chemistry be held responsible for any errors or omissions in this *Accepted Manuscript* or any consequences arising from the use of any information it contains.

1  
2  
3  
4  
5  
6  
7 **1 Optimization of double spike technique using peak jump collection by**  
8  
9  
10 **2 Monte Carlo method: an example for the determination of Ca isotope**  
11  
12 **3 ratios**

13  
14  
15 4 Lanping Feng<sup>a</sup>, Lian Zhou<sup>\*a</sup>, Lu Yang<sup>b</sup>, Shuoyun Tong<sup>a</sup>, Zhaochu Hu<sup>a</sup> and Shan Gao<sup>a</sup>  
16

17  
18 <sup>a</sup> State Key Laboratory of Geological Processes and Mineral Resources, School of Earth  
19  
20 Sciences, China University of Geosciences, Wuhan 430074, China  
21

22  
23 <sup>b</sup> Chemical Metrology, National Research Council Canada, Ottawa, Ontario, K1A 0R6,  
24  
25  
26 Canada  
27

28  
29 9

30  
31 \*Corresponding author  
32

33  
34 E-mail: zhcug@163.com  
35

36  
37 Tel: 86-27-67883932  
38

39  
40 Fax: 86-27-67885096  
41

42  
43 14

44  
45 15

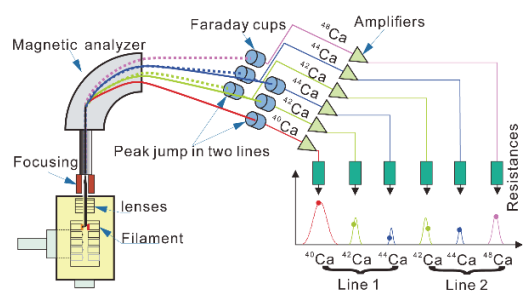
46 ***Submitted to Journal of Analytical Atomic Spectrometry***  
47

48  
49 17  
50  
51  
52  
53  
54  
55  
56  
57  
58  
59  
60

18 **Content entry**

19 Monte Carlo method is used to estimate the additional uncertainty of measured value  
20 introduced by peak jump mode for Ca isotope ratios determination.

21



24 **Abstract**

25 Three important factors, including the choice of an appropriate spike isotope pair, the  
26 composition of double spike, and the ratio of double spike to sample, have been proven to  
27 have significant effect on the precision of the double spike technique. Moreover, peak jump  
28 (i.e., dynamic) collection mode is frequently used, which could lead to more variable  
29 parameters such as cup configurations, ratio combinations and integration times in different  
30 jump lines. In order to optimize the above conditions under the peak jump mode, a Monte  
31 Carlo method that simulates uncertainties from Johnson noise and counting statistics is  
32 applied for the prediction of the precisions of measured results using double spike  
33 technique. As an example, this model was used to predict the possibility for cup  
34 configurations and ratio combinations of three double spike pairs of  $^{42}\text{Ca}$ - $^{48}\text{Ca}$ ,  $^{43}\text{Ca}$ - $^{48}\text{Ca}$   
35 and  $^{46}\text{Ca}$ - $^{48}\text{Ca}$ , respectively, in two jump lines. Predicted internal precisions improved 25%,  
36 20% and 25% by using  $^{42}\text{Ca}$ - $^{48}\text{Ca}$ ,  $^{43}\text{Ca}$ - $^{48}\text{Ca}$  and  $^{46}\text{Ca}$ - $^{48}\text{Ca}$  double spike, respectively,  
37 under optimized conditions. The theoretical predicted optimum precision was verified by  
38 repeatedly measuring two standards of NIST SRM 915a and NIST SRM 915b using  $^{42}\text{Ca}$ -  
39  $^{48}\text{Ca}$  double spike over several months. The observed internal precisions of  $\delta^{44}\text{Ca}$  in these  
40 two standards are in good agreement with the predicted internal precisions, validating the  
41 effectiveness of the proposed Monte Carlo technique. The observed external precisions in  
42 two standards are 8-9 times poorer than the internal precisions, properly due to an extra  
43 uncertainty source. Nevertheless, the optimal ratio combination yields the best external

1  
2  
3  
4  
5  
6  
7 44 precision. As demonstrated, the proposed Monte Carlo simulation is an effective method  
8  
9  
10 45 to predict the optimal cup configurations, ratio combinations and integration times for  
11  
12 46 double spike technique using peak jump collection mode.  
13  
14

15 47

16  
17  
18 48 **Keywords:** Double spike technique, Monte Carlo simulation technique, Peak jump  
19  
20  
21 49 collection mode  
22

23 50  
24  
25  
26  
27  
28  
29  
30  
31  
32  
33  
34  
35  
36  
37  
38  
39  
40  
41  
42  
43  
44  
45  
46  
47  
48  
49  
50  
51  
52  
53  
54  
55  
56  
57  
58  
59  
60

1  
2  
3  
4  
5  
6  
7 **51 Introduction**  
8

9  
10 52 Double spike technique is widely used for the determination of non-traditional stable  
11  
12 53 isotopic compositions of natural samples. Natural variation in non-traditional stable  
13  
14  
15 54 isotopic composition is usually small, for example only about 4‰ for  $\delta^{44}\text{Ca}^{1,2}$  and 6.4%  
16  
17  
18 55 for  $\delta^{98}\text{Mo}^3$ . Thus, characterization of non-traditional stable isotope demands the most  
19  
20  
21 56 accurate and precise double spike technique to investigate these small isotopic differences  
22  
23  
24 57 in natural samples. The double spike technique was established by the early works of  
25  
26  
27 58 Dodson.<sup>4,5</sup> It is a solution that could solve the instrumental and natural fractionation of  
28  
29  
30 59 samples simultaneously with use of three isotope ratios constructed from the abundance of  
31  
32  
33 60 four isotopes in double spike, sample and mixture, respectively.<sup>6</sup> Great efforts have been  
34  
35  
36 61 made in the last decade to improve the accuracy and precision of this technique. It has been  
37  
38  
39 62 verified that the choice of an appropriate double spike isotope pair, the composition of  
40  
41  
42 63 double spike, and the proportion of double spike in the mixture are the key factors to  
43  
44  
45 64 dominate the precision of the double spike technique.<sup>7-9</sup> Meanwhile, the optimum double  
46  
47  
48 65 spike predicted by theoretical models have been successfully used in various practical  
49  
50  
51 66 applications. The term optimum double spike collectively refers to the optimum choice of  
52  
53  
54 67 the double spike isotope pair, the composition of double spike, and the proportion of double  
55  
56  
57 68 spike in the mixture. For example, Rudge *et al.*<sup>7</sup> firstly reported theoretical optimum double  
58  
59  
60 69 spikes for 33 elements, which were confirmed by a good agreement between the predicted  
and observed value of  $\delta^{56}\text{Fe}$  ratio measurements. Subsequently, John *et al.*<sup>8</sup> further

1  
2  
3  
4  
5  
6  
7 71 improved the precision up to 30% for double spike-MC-ICPMS (DS-MC-ICPMS)  
8  
9  
10 72 technique by using an independent variation of sample and double spike concentration, and  
11  
12 73 successfully predicted the optimal proportion of double spike in mixture for the  
13  
14 74 determination of  $\delta^{56}\text{Fe}$ ,  $\delta^{66}\text{Zn}$  and  $\delta^{114}\text{Cr}$ . Moreover, Lehn *et al.*<sup>9</sup> optimized the  $^{42}\text{Ca}$ - $^{43}\text{Ca}$   
15  
16 75 double spike by not only considering the optimal double spike, but also taking the Faraday  
17  
18 76 cup deterioration effect into account when utilizing double spike TIMS (DS-TIMS)  
19  
20  
21 77 analysis for Ca isotope ratios, and achieved an excellent external precision of  $\sim 0.04\%$  ( $2\sigma$ )  
22  
23 78 for  $\delta^{44}\text{Ca}$ . Clearly, prediction of the precision of measurements is useful to understand the  
24  
25  
26 79 complex uncertainty propagation process of double spike technique.  
27  
28  
29  
30

31  
32 80 In previous studies,<sup>7-8</sup> all isotopes were considered being collected simultaneously in  
33  
34 81 their predicted models and confirmed by practical applications which were implemented  
35  
36 82 under static collection mode. However, peak jump collection mode (i.e., dynamic) is often  
37  
38 83 used for the implementation of double spike technique,<sup>10-14</sup> which leads to more variable  
39  
40 84 parameters such as cup configurations, ratio combinations and independent integration  
41  
42  
43 85 times in different magnetic jump lines. Lehn *et al.*<sup>9</sup> first introduced peak jump collection  
44  
45 86 model into their prediction model for precision, but these parameters were not fully  
46  
47  
48 87 explored due to concerns about possible damage of collectors.  
49  
50  
51

52  
53 88 In this study, a Monte Carlo technique that simulates uncertainties from Johnson noise  
54  
55 89 and counting statistic following the optimization model presented in the previous studies<sup>7-</sup>  
56  
57  
58 90 <sup>9</sup> was used to estimate measurement precisions of variable cup configurations, ratio  
59  
60

1  
2  
3  
4  
5  
6  
7 91 combinations and integration times under peak jump collection mode. Three Ca double  
8  
9  
10 92 spike pairs:  $^{42}\text{Ca}$ - $^{48}\text{Ca}$ ,  $^{43}\text{Ca}$ - $^{48}\text{Ca}$  and  $^{46}\text{Ca}$ - $^{48}\text{Ca}$  were investigated using the above Monte  
11  
12  
13 93 Carlo simulation technique, to discover how these instrument setting parameters impact on  
14  
15 94 the analysis precision, and find out the optimum settings for these parameters. These double  
16  
17  
18 95 spike pairs were chosen because of the large mass dispersion between isotopes  $^{40}\text{Ca}$  and  
19  
20  
21 96  $^{48}\text{Ca}$ , which cannot be collected simultaneously. The feasibility of this estimation model  
22  
23  
24 97 was verified by the determination of standards spiked with  $^{42}\text{Ca}$ - $^{48}\text{Ca}$  double spikes. The  
25  
26  
27 98 observed internal and external precisions of the  $\delta^{44}\text{Ca}$  ratio of two standards of NIST SRM  
28  
29  
30 99 915a and NIST SRM 915b were compared with the predicted precisions, respectively.

100

**101 Precision prediction model****102 Uncertainty sources**

103 There are two different quantifiable uncertainties during data collection by TIMS, which  
104 can induce the uncertainty of measured value of individual isotope: one is Johnson noise  
105 associated with the detector, also known as 'hot noise'; and the other is counting statistics  
106 of the ion beam, also known as 'shot noise'. The variation of individual isotope is normally  
107 distributed within a standard deviation of the stochastic uncertainty with a mean value of  
108 its real intensity. According to the previous reports,<sup>7-9</sup> Johnson noise is only related to the  
109 integration time when the resistance ( $R$ ) associated with the amplifier is specified. The  
110 absolute uncertainty due to Johnson noise can be expressed in Eq. 1:<sup>7-9</sup>



$$\sigma_{Johnson\ noise}^i = \sqrt{\frac{4kTR}{\Delta t_i}} \quad (1)$$

where  $k$  is Boltzmann constant of  $1.3806504 \times 10^{-23}$  J K<sup>-1</sup>,  $i$  is the label of the 4 isotopes involved in the inversion ( $i = 1, 2, 3$  or  $4$ ),  $T$  is the temperature of the amplifier at 300 K,  $R$  is the resistance associated with amplifier, defaulted by  $10^{11}$   $\Omega$  (consistent with instrumental setting) and  $\Delta t_i$  is the integration time. The absolute uncertainty due to counting statistics is expressed in Eq. 2:<sup>7-9</sup>

$$\sigma_{counting\ statistics}^i = \sqrt{\frac{eRV_i}{\Delta t_i}} \quad (2)$$

where  $e$  is the elementary charge of  $1.602176487 \times 10^{-19}$  C and  $V_i$  is the ion beam intensity.

Finally, the uncertainty associated with each measured individual isotope is:

$$\sigma_{uncert}^i = \sqrt{(\sigma_{Johnson\ noise}^i)^2 + (\sigma_{counting\ statistics}^i)^2} \quad (3)$$

### Uncertainty propagation

The uncertainty model indicates that the uncertainty of signal intensity of each isotope is associated with the ion beam intensity ( $V_i$ ) and the integration time ( $\Delta t_i$ ). The mean total ion beam intensity ( $V$ ) is defined as the sum intensity of the involved four isotopes. Individual isotope intensity ( $V_i$ ) is related to its abundance in the mixture, which in turn to the composition of spike and the proportion of spike in the mixture. The composition of double spike (T) is calculated by the proportion of two single spikes (PSA, PSB) as the following equation:

$$T_i = q \times PSA_i + (1 - q) \times PSB_i \quad (4)$$

where  $q$  is the proportion of  $PSA_i$  in double spike,  $PSA_i$  and  $PSB_i$  are the abundance of isotope  $i$  in PSA and PSB, respectively. Similarly, the composition of mixture (M) can be calculated by the proportion of double spike and sample (N):

$$M_i = p \times T_i + (1 - p) \times N_i \quad (5)$$

where  $p$  is the proportion of the double spike in the mixture and  $N_i$  is the abundance of isotope  $i$  in the sample. Here the ‘‘Russell value’’<sup>15</sup> (Table. 1) was adopted as the initiate sample composition ( $N_i$ ) for the double spike iteration. The intensity of each of the four isotopes ( $V_i$ ) can be calculated by its relative abundance and the sum abundance of these four isotopes in the mixture as the following equation:

$$V_i = VM_i \frac{1}{\sum_i M_i} \quad (6)$$

The uncertainty of signal intensity of each isotope is calculated by using  $\sigma_{error}^i$  multiplying by a random number of  $R_{nom}$ , which is normally distributed with a mean value of 0 and a standard deviation of 1. Thus, the measured signal intensity of each isotope can be simulated by adding this uncertainty to its real value:

$$V_M^i = V_i + \sigma_{uncert}^i R_{nom} \quad (7)$$

Under static collection model, every isotope is only measured once and can be simply simulated by the above equations. However, it is more complicated when peak jump mode is used. Although the measured values of the same isotope in different lines are from the

1  
2  
3  
4  
5  
6  
7 149 same ion beam (have equal  $V_i$ ), they are independent of each other for the stochastic  
8  
9  
10 150 uncertainties. Consequently, these independent measured values (IMVs) that were  
11  
12 151 measured in different lines have independent uncertainties. According to Eqs. (1), (2), (3),  
13  
14  
15 152 and (7), IMVs can be simulated by using independent  $\Delta t_i$  and  $R_{nom}$ , respectively, while  
16  
17  
18 153 using the same  $V_i$ , since they were from same ion beam but measured in different lines.  
19

20 154

### 21 155 **Monte Carlo uncertainty estimation**

22  
23  
24 156 For double spike calculation, three ratios constructed from the measured values of four  
25  
26 157 isotopes can be solved by either algebraic<sup>7</sup> or iterative<sup>9, 10</sup> approach to obtain the natural  
27  
28 158 composition of the sample. As described above, under static collection mode each isotope  
29  
30 159 was only measured once, with no extra measurement uncertainty. As a result, only one  
31  
32 160 combination of three isotope ratios is needed for the double spike calculation ratios  
33  
34  
35 161 constructed from only four measured values, and any isotope can be used as the  
36  
37  
38 162 denominator. When peak jump collection mode is used, additional uncertainty is brought  
39  
40  
41 163 by IMVs compared to those measured under static collection mode. It is clear that the cup  
42  
43 164 configuration determines which isotope can have IMVs, while the ratio combination  
44  
45  
46 165 determines the uncertainty of which IMVs will pass through the uncertainty propagation  
47  
48  
49 166 procedure. Thus different cup configurations and ratio combinations can be simulated by  
50  
51  
52 167 using different IMVs to construct three ratios. In this study three double spike pairs: <sup>42</sup>Ca-

1  
2  
3  
4  
5  
6  
7 168  $^{48}\text{Ca}$ ,  $^{43}\text{Ca}$ - $^{48}\text{Ca}$  and  $^{46}\text{Ca}$ - $^{48}\text{Ca}$  were investigated to demonstrate the simulation procedure  
8  
9  
10 169 of different cup configurations and ratio combinations by using IMVs.

11  
12 Because of the complexity in solving the double spike calculation and in the estimation  
13  
14  
15 171 of the precision of  $\delta^{44}\text{Ca}$  ratio, Monte Carlo technique was applied to simulate the  
16  
17  
18 172 uncertainty propagation. In this study, Monte Carlo technique was carried out in an Excel  
19  
20  
21 173 spreadsheet. Once three Ca ratios required for double spike calculation are identified,  
22  
23  
24 174 different double spike data reduction approaches generate the same  $\delta^{44}\text{Ca}$  value. Here we  
25  
26  
27 175 adopted the equation presented in Lehn *et al.*<sup>9</sup> to calculate double spike iteration. For the  
28  
29  
30 176 purpose of obtaining accurate simulate results, 5000 simulated analyses were used in each  
31  
32  
33 177 simulation. At this level, the variation of predict results of  $\delta^{44}\text{Ca}$  was less than 0.005%  
34  
35  
36 178 (one standard deviation). The internal precision was determined by doubling the standard  
37  
38  
39 179 error of the mean result ( $2\sigma_{\text{SEM}}$ ), with the assumption of 100 data scans as actual  
40  
41  
42 180 measurements.

43 181

## 44 45 182 **Experimental**

### 46 47 48 183 **Instrumentation**

49  
50  
51 184 All Ca isotope measurements were performed on a Triton TIMS (Thermo Finnigan,  
52  
53  
54 185 Bremen, Germany) at the State Key Laboratory of Geological Processes and Mineral  
55  
56  
57 186 Resources in China University of Geosciences, Wuhan. This instrument is equipped with  
58  
59  
60 187 nine Faraday cups connected with nine rotatable virtual amplifiers which help eliminate

1  
2  
3  
4  
5  
6  
7 188 gain calibration biases. The resistor of each amplifier is  $10^{11} \Omega$  as default. Rhenium filaments  
8  
9  
10 189 assemblies were outgassed at 1 A for one hour, and then at 4 A for another hour at a  $10^{-6}$   
11  
12 190 mbar condition.

### 15 191 **Reagents and samples**

16  
17  
18 192 Nitric acid was purified in-house prior to use by sub-boiling distillation of reagent grade  
19  
20 193 feedstock in a DST-1000 acid purification system (Savillex, Eden Prairie, USA). 20%  
21  
22 194  $H_3PO_4$  used to load sample was prepared by dilution of Suprapur<sup>®</sup> grade ortho-Phosphoric  
23  
24 195 acid (Merck KGaA, Darmstadt, Germany) with deionized water. All the dilutions and  
25  
26 196 cleaning procedures were carried out with deionized Milli-Q water (Millipore, Billerica  
27  
28  
29 197 MA, USA). Two Ca carbonate powder isotopic reference materials, NIST SRM 915a and  
30  
31  
32 198 NIST SRM 915b, were purchased from the National Institute of Standards and Technology  
33  
34  
35 199 (NIST, Gaithersburg MD, USA). The total Ca blank was typically less than 10ng, negligible  
36  
37  
38 200 compared to the amount of Ca processed.

### 41 201 **Analysis of Ca isotopes**

42  
43  
44 202 Filament loading protocol from Holmden *et al.*<sup>16</sup> and Lehn *et al.*<sup>9</sup> was followed. Instead of  
45  
46 203 using single filament, double filaments arrangement was adopted to achieve lower mass  
47  
48 204 fractionation and more stable ion beams.<sup>17</sup> In brief, a current of 1.4 A was passed through  
49  
50 205 the filament, and Parafilm<sup>TM</sup> was gently swiped on either side of the filament, helping  
51  
52 206 constrain the sample droplet. Then 1  $\mu$ L of spiked sample solution containing 3  $\mu$ g Ca was  
53  
54  
55 207 carefully loaded onto the centre of the filament in three droplets. After all the droplets were  
56  
57  
58  
59  
60

1  
2  
3  
4  
5  
6  
7 208 dried at 1 A, 1  $\mu\text{L}$  of 20%  $\text{H}_3\text{PO}_4$  was loaded on the filament, and the mixture droplet was  
8  
9  
10 209 dried at 1.6 A. Finally, the electrical current was increased until a weak red glow was visible,  
11  
12 210 followed by shutting down of the electrical current.

13  
14  
15 211 Ca isotopes intensities were acquired in peak jump mode for all spiked samples using  
16  
17 212 the cup configuration listed in Table 2. The sample heating was performed using an  
18  
19 213 automated heating program, allowing fully automated measurements. Intensity of  $^{40}\text{Ca}$  was  
20  
21 214 maintained at about 9 V to achieve 10 V of total ( $^{40}\text{Ca}$ ,  $^{42}\text{Ca}$ ,  $^{44}\text{Ca}$  and  $^{48}\text{Ca}$ ) signal intensity.  
22  
23 215 Detailed instrument settings for the measurements are listed in Table 2.  
24  
25  
26  
27  
28  
29  
30  
31

## 32 217 **Results and discussion**

### 33 34 218 **Effect of cup configuration and ratio combination**

35  
36  
37 219 There is a large mass dispersion in Ca isotopes, i.e., 20% relative mass dispersion for  $^{40}\text{Ca}$   
38  
39 220 to  $^{48}\text{Ca}$ , which exceeds the limitation of most modern multi-collector mass spectrometry.

40  
41  
42 221 Therefore, six Ca isotopes ranging from the lowest mass  $^{40}\text{Ca}$  to the highest mass  $^{48}\text{Ca}$   
43  
44 222 cannot be collected simultaneously. An alternative is to separate Ca isotopes into two lines  
45  
46 223 by collecting  $^{40}\text{Ca}$  to  $^{46}\text{Ca}$  in the low mass line first and collecting  $^{42}\text{Ca}$  to  $^{48}\text{Ca}$  in the high  
47  
48 224 mass line using peak jump method (Fig. 1). For example, peak jump collection using two  
49  
50 225 lines was employed with use of  $^{42}\text{Ca}$ - $^{48}\text{Ca}$  double spike<sup>11, 18</sup> or  $^{43}\text{Ca}$ - $^{48}\text{Ca}$  double spike<sup>10, 19</sup>.

51  
52  
53 226 Although the use of double spike pair of  $^{46}\text{Ca}$ - $^{48}\text{Ca}$  has not been reported, measurements  
54  
55  
56 227 are still possible by using two lines peak jump collection mode. Consequently, IMVs of  
57  
58  
59  
60

1  
2  
3  
4  
5  
6  
7 228  $^{42}\text{Ca}$ ,  $^{43}\text{Ca}$ ,  $^{44}\text{Ca}$  and  $^{46}\text{Ca}$  generate many possibilities of cup configurations and ratio  
8  
9  
10 229 combinations. Under two peak jump lines, there are up to two different isotopes having  
11  
12 230 IMVs for each double spike pair. Note that when ratios are constructed from different lines,  
13  
14  
15 231 additional uncertainties may arise from signal fluctuations (through quadratic drift  
16  
17 232 correction), contributing extra uncertainties to the measured precision of  $\delta^{44}\text{Ca}$ . In this  
18  
19 233 study, only ratios constructed from the same line are considered for the estimation.  
20  
21  
22 234 Therefore, no more than five measured values of four isotopes can be used to construct  
23  
24  
25 235 three ratios, and IMVs of two isotopes (e.g.  $^{42}\text{Ca}$  and  $^{44}\text{Ca}$ ) cannot be employed to construct  
26  
27 236 ratios at the same time.

30  
31 237 Our original objective was to identify the most effective conditions for Ca isotope  
32  
33 238 ratios determination among these various cup configurations and ratio combinations. To  
34  
35 239 achieve this, we listed all the potential cup configurations, including five collectors in two  
36  
37 240 lines (Fig. 1 a, b, c and d). Correspondingly, there were four different ratio combinations  
38  
39 241 utilizing different IMVs: (A<sub>1</sub>-A<sub>3</sub>)  $^{40}\text{Ca}_{\#1}/^{4i}\text{Ca}_{\#1}$ ,  $^{44}\text{Ca}_{\#1}/^{4i}\text{Ca}_{\#1}$ ,  $^{48}\text{Ca}_{\#2}/^{4i}\text{Ca}_{\#2}$  ( $i = 2, 3$  or  $6$ );  
40  
41 242 (B<sub>1</sub>-B<sub>3</sub>)  $^{40}\text{Ca}_{\#1}/^{4i}\text{Ca}_{\#1}$ ,  $^{44}\text{Ca}_{\#2}/^{4i}\text{Ca}_{\#2}$ ,  $^{48}\text{Ca}_{\#2}/^{4i}\text{Ca}_{\#2}$ ; (C<sub>1</sub>-C<sub>3</sub>)  $^{40}\text{Ca}_{\#1}/^{44}\text{Ca}_{\#1}$ ,  $^{4i}\text{Ca}_{\#1}/^{44}\text{Ca}_{\#1}$ ,  
42  
43 243  $^{48}\text{Ca}_{\#2}/^{44}\text{Ca}_{\#2}$ ; (D<sub>1</sub>-D<sub>3</sub>)  $^{40}\text{Ca}_{\#1}/^{44}\text{Ca}_{\#1}$ ,  $^{4i}\text{Ca}_{\#2}/^{44}\text{Ca}_{\#2}$ ,  $^{48}\text{Ca}_{\#2}/^{44}\text{Ca}_{\#2}$ . For the purpose of the  
44  
45  
46 244 acquisition of optimal cup configuration and ratio combination, Monte Carlo technique was  
47  
48 245 used. Measurement internal precisions were predicted for 8s of integration time for each  
49  
50  
51 246 line and 10V for the total signal intensity using A-D ratio combinations. Static collection  
52  
53  
54 247 mode was investigated using ratio combinations: (E<sub>1</sub>-E<sub>3</sub>)  $^{40}\text{Ca}_{\#1}/^{44}\text{Ca}_{\#1}$ ,  $^{4i}\text{Ca}_{\#1}/^{44}\text{Ca}_{\#1}$ ,  
55  
56  
57  
58  
59  
60

1  
2  
3  
4  
5  
6  
7 248  $^{48}\text{Ca}_{\#1}/^{44}\text{Ca}_{\#1}$ , in order to compare to those of peak jump collection mode. The predicted  
8  
9  
10 249 internal precisions ( $2\sigma_{\text{SEM}}$ ) of  $\delta^{44}\text{Ca}$  values using  $^{42}\text{Ca}$ - $^{48}\text{Ca}$ ,  $^{43}\text{Ca}$ - $^{48}\text{Ca}$  and  $^{46}\text{Ca}$ - $^{48}\text{Ca}$   
11  
12  
13 250 double spike pairs are shown in Fig. 2 respectively.

14  
15 251 Our results showed that with use of any double spike pair of  $^{42}\text{Ca}$ - $^{48}\text{Ca}$ ,  $^{43}\text{Ca}$ - $^{48}\text{Ca}$  and  
16  
17  
18 252  $^{46}\text{Ca}$ - $^{48}\text{Ca}$ , the predicted internal precisions of  $\delta^{44}\text{Ca}$  of peak jump collection varied from  
19  
20  
21 253 those of static collection. The best predicted internal precisions of  $\delta^{44}\text{Ca}$ , using  $^{42}\text{Ca}$ - $^{48}\text{Ca}$ ,  
22  
23 254  $^{43}\text{Ca}$ - $^{48}\text{Ca}$  and  $^{46}\text{Ca}$ - $^{48}\text{Ca}$  double spikes and peak jump collection for Ca ratios using  
24  
25  
26 255 configurations of C<sub>1</sub>, A<sub>2</sub> and D<sub>3</sub>, were improved by 20%, 25% and 10%, respectively,  
27  
28  
29 256 compared to those estimated by using static mode E<sub>1</sub>, E<sub>2</sub> and E<sub>3</sub>. These results indicated  
30  
31  
32 257 that the additional uncertainties generated by using peak jump collection mode had an  
33  
34  
35 258 impact on the predicted internal precision of  $\delta^{44}\text{Ca}$ . However, optimal double spike areas  
36  
37  
38 259 did not change significantly between peak jump and static collection mode in nearly all  
39  
40  
41 260 cases. Thus, the optimal double spike estimated under static collection mode condition is  
42  
43  
44 261 suitable for measurements operated under peak jump collection mode.

45 262 On the other hand, the optimal cup configuration and ratio combination is different for  
46  
47  
48 263 individual double spike pair. With the use of  $^{42}\text{Ca}$ - $^{48}\text{Ca}$  double spike, the best predicted  
49  
50  
51 264 internal precision of  $\delta^{44}\text{Ca}$  can be obtained by using C<sub>1</sub> ratio combination (i.e.,  $^{40}\text{Ca}_{\#1}/^{44}\text{Ca}_{\#1}$ ,  
52  
53 265  $^{42}\text{Ca}_{\#1}/^{44}\text{Ca}_{\#1}$ ,  $^{48}\text{Ca}_{\#2}/^{44}\text{Ca}_{\#2}$ ). This ratio combination indicates that the best cup  
54  
55  
56 266 configuration with use of  $^{42}\text{Ca}$ - $^{48}\text{Ca}$  double spike should be ranged for measurements of  
57  
58  
59 267  $^{40}\text{Ca}$ ,  $^{42}\text{Ca}$ , and  $^{44}\text{Ca}$  in the first line and only  $^{44}\text{Ca}$  and  $^{48}\text{Ca}$  in the second line. Similarly,  
60



1  
2  
3  
4  
5  
6  
7 268 for  $^{43}\text{Ca}$ - $^{48}\text{Ca}$  double spike, the best predicted internal precision can be obtained by using  
8  
9  
10 269 the ratio combination A<sub>2</sub> (i.e.,  $^{40}\text{Ca}_{\#1}/^{43}\text{Ca}_{\#1}$ ,  $^{44}\text{Ca}_{\#1}/^{43}\text{Ca}_{\#1}$ ,  $^{48}\text{Ca}_{\#2}/^{43}\text{Ca}_{\#2}$ ) and measuring  
11  
12 270  $^{40}\text{Ca}$ ,  $^{43}\text{Ca}$  and  $^{44}\text{Ca}$ , and  $^{43}\text{Ca}$  and  $^{48}\text{Ca}$  in the first and second lines, respectively. For  $^{46}\text{Ca}$ -  
13  
14  
15 271  $^{48}\text{Ca}$  double spike, the best predicted internal precision can be obtained by using the ratio  
16  
17  
18 272 combination D<sub>3</sub> (i.e.,  $^{40}\text{Ca}_{\#1}/^{44}\text{Ca}_{\#1}$ ,  $^{46}\text{Ca}_{\#2}/^{44}\text{Ca}_{\#2}$ ,  $^{48}\text{Ca}_{\#2}/^{44}\text{Ca}_{\#2}$ ) and measuring  $^{40}\text{Ca}$ ,  $^{44}\text{Ca}$ ,  
19  
20  
21 273 and  $^{44}\text{Ca}$ , and  $^{46}\text{Ca}$  and  $^{48}\text{Ca}$  in the first and second lines, respectively. By contrast, improper  
22  
23  
24 274 selection of cup configuration and ratio combination can sharply decrease the predicted  
25  
26  
27 275 internal precision of  $\delta^{44}\text{Ca}$ . For example, B<sub>1</sub>, D<sub>2</sub> and C<sub>3</sub> combination decreased the internal  
28  
29  
30 276 precision by 25%, 20%, and 25%, respectively, compared to that obtained using optimum  
31  
32  
33 277 combination of C<sub>1</sub>, A<sub>2</sub> and D<sub>3</sub>. Moreover, as shown in Figure 2-C<sub>3</sub>, the optimum area  
34  
35  
36 278 (optimum ranges of composition of double spike and proportion of double spike in the  
37  
38  
39 279 mixture) changes significantly when improper selection of cup configurations and ratio  
40  
41  
42 280 combinations is made.

43  
44  
45 281 It is clear from the above results that the selection of cup configuration and ratio  
46  
47  
48 282 combination has a significant impact on the predicted precision of  $\delta^{44}\text{Ca}$ . The large  
49  
50  
51 283 difference in the predicted internal precision between simulations under peak jump and  
52  
53  
54 284 under static collection mode suggests that the additional uncertainties arising from IMVs  
55  
56  
57 285 not only reduce the precision of  $\delta^{44}\text{Ca}$ , but also have complex effects on uncertainty  
58  
59  
60 286 propagation. Moreover, the combinations of IMVs have a significant impact on the  
287  
288  
289 287 predicted internal precision of  $\delta^{44}\text{Ca}$ , even with use of the same group of standard

1  
2  
3  
4  
5  
6  
7 288 uncertainties. Thus, all possible cup configurations, ratio combinations, and IMVs used to  
8  
9 289 construct ratios should be fully investigated under the actual analysis conditions, such as  
10  
11 290 the number of Faraday cups, peak jump lines and mass dispersion of isotopes. Based on  
12  
13 291 Monte Carlo prediction, the optimum IMVs of Ca isotopes to generate three Ca ratios can  
14  
15 292 be identified, resulting in significant improvements on the predicted precision of  $\delta^{44}\text{Ca}$ .  
16  
17  
18  
19  
20

### 21 **Effect of integration time**

22  
23 294 Compared to static collection mode, peak jump mode brings in variable  $\Delta t_i$  in different  
24  
25 295 lines. Independent variation of integration times on each line also has an impact on the  
26  
27 296 precision. With the proposed Monte Carlo method, internal precision was predicted by  
28  
29 297 changing integration time of line1 ( $\Delta t_1$ ) and line2 ( $\Delta t_2$ ), separately, under  $A_1$ - $D_1$   
30  
31 298 combinations for  $^{42}\text{Ca}$ - $^{48}\text{Ca}$  double spike, while keeping a fixed total integration time ( $\Delta t$ )  
32  
33 299 of 16s (Fig. 3a). Predicted internal precision of  $\delta^{44}\text{Ca}$  showed a significant variation with  
34  
35 300 use of independent  $\Delta t_1$  and  $\Delta t_2$ , compared to that use of  $\Delta t_1 = \Delta t_2$  under fixed total  $\Delta t$ . As  
36  
37 301 shown in Fig. 3a, the optimum cup configuration and ratio combination ( $C_1$ ) predicted  
38  
39 302 above (with use of  $\Delta t_1 = \Delta t_2 = 8\text{s}$ ) generated the most precise results compared to  $A_1$ ,  $B_1$  and  
40  
41 303  $D_1$  conditions, while each condition using optimal  $\Delta t_1$  and  $\Delta t_2$ , respectively. Therefore, the  
42  
43 304 optimum cup configuration and ratio combination is a robust choice under both equal and  
44  
45 305 independent integration times for different lines with use of  $^{42}\text{Ca}$ - $^{48}\text{Ca}$  double spike, and  
46  
47 306 this is also true for  $^{43}\text{Ca}$ - $^{48}\text{Ca}$  and  $^{46}\text{Ca}$ - $^{48}\text{Ca}$  double spikes.  
48  
49  
50  
51  
52  
53  
54  
55  
56  
57

58  
59 307 Furthermore, the relationship between predicted internal precision and independent  $\Delta t_i$   
60

1  
2  
3  
4  
5  
6  
7 308 and  $\Delta t_2$  can be used to reduce the difference of ion count per sample in different lines. For  
8  
9  
10 309 example,  $^{40}\text{Ca}$  is about 40 times more abundant than  $^{44}\text{Ca}$ , and 20 times more abundant  
11  
12 310 than  $^{48}\text{Ca}$  in spiked samples with use of optimal  $^{42}\text{Ca}$ - $^{48}\text{Ca}$  double spike. In the case of  
13  
14  
15 311 similar predicted internal precision, using  $\Delta t_1=4$  and  $\Delta t_2=12$ , respectively can narrow this  
16  
17  
18 312 gap by 3 times compared to using  $\Delta t_1=\Delta t_2=8$  under C<sub>1</sub> configuration. Total integration  
19  
20 313 times of 16s were experimentally tested using  $\Delta t_1=4$  and  $\Delta t_2=12$  (Fig. 3a). It is evident that  
21  
22  
23 314 experimental results lie fairly close to the predicted curve, confirming the feasibility of  
24  
25  
26 315 Monte Carlo method for the internal precision estimation with use of independent  
27  
28  
29 316 integration time in different lines.

30  
31 317 On the other hand, peak jump mode is a time-consuming method relative to static mode.  
32  
33  
34 318 The uncertainty model indicates that the uncertainty of signal intensity of each isotope is  
35  
36  
37 319 largely dependent on the integration time. Conceptually, the longer the integration time,  
38  
39  
40 320 the more precise the results. As shown in Fig. 3b, for  $^{42}\text{Ca}$ - $^{48}\text{Ca}$  double spike with A1-  
41  
42  
43 321 E1 configurations, the predicted internal precisions of  $\delta^{44}\text{Ca}$  increase significantly as total  
44  
45  
46 322 integration time increases from 2s to 16s, and then only slightly increase at higher  
47  
48  
49 323 integration times. Unfortunately, integration time is a major limitation for high sample  
50  
51  
52 324 throughput analysis since the sample heating procedure is relatively constant. Analysis time  
53  
54  
55 325 is doubled when peak jump collection mode is applied. Total integration time of 16s ( $\Delta t_1 =$   
56  
57  
58 326  $\Delta t_2=8$ ) was chosen to achieve high precision Ca isotope ratio measurements while  
59  
60 327 maintaining relatively high sample throughput in this study.

1  
2  
3  
4  
5  
6  
7 3288 **329 Validation of Monte Carlo prediction**

9  
10 330 NIST SRM 915a and NIST SRM 915b standard solutions were spiked with  $^{42}\text{Ca}$ - $^{48}\text{Ca}$   
11  
12 331 double spike for the  $\delta^{44}\text{Ca}$  measurements to validate Monte Carlo method for precision  
13  
14  
15 332 prediction. The  $^{42}\text{Ca}$ - $^{48}\text{Ca}$  double spike was prepared from two single spikes of  $^{42}\text{Ca}$   
16  
17  
18 333 (94.49%) and  $^{48}\text{Ca}$  (97.80%) (Table 1). Since the difference between the real and the pure  
19  
20  
21 334 (100%) single spikes in predicted results was smaller than the accuracy of Monte Carlo  
22  
23  
24 335 technique under 5000 simulations, the composition of double spike and the proportion of  
25  
26  
27 336 double spike in the mixture were prepared following the optimal predicted results (Fig. 2  
28  
29  
30 337 C<sub>1</sub>). The composition of the  $^{42}\text{Ca}$ - $^{48}\text{Ca}$  double spike was calibrated against the NIST 915a  
31  
32  
33 338 by subtracting the standard from the mixture using a reverse process that calculates sample  
34  
35  
36 339 compositions. Thus, all the  $\delta^{44}\text{Ca}$  reported in this paper were relative to NIST SRM 915a.  
37  
38  
39 340 These two spiked standard solutions were directly analyzed without chemical separation  
40  
41  
42 341 process. Therefore, uncertainty sources were limited in instrumental analysis process. The  
43  
44  
45 342 ion beams of  $^{42}\text{Ca}$  and  $^{44}\text{Ca}$  were collected in every line to simulate all the potential cup  
46  
47  
48 343 configurations (A<sub>1</sub>-D<sub>1</sub>) under two lines measurement (Table 2). Total of 81 data points were  
49  
50  
51 344 obtained with each data point representing the result of a single run session of 100 scans  
52  
53  
54 345 (10 blocks  $\times$  10 cycles). Internal precision and external precision from these data were then  
55  
56  
57 346 compared with the results predicted using Monte Carlo simulation.

58  
59  
60 347 Results of measured internal precision ( $2\sigma_{\text{SEM}}$ ) of  $\delta^{44}\text{Ca}$  using different Ca ratio

1  
2  
3  
4  
5  
6  
7 348 combinations are presented in Fig. 4. Overall, observed and predicted internal precision are  
8  
9  
10 349 in good agreement, but 10-17 data points showed irregular fractionation trends during  
11  
12  
13 350 measurements, mainly due to a poor sample loading process wherein sample was spread  
14  
15 351 on the filament and resulted in erratic patterns of fractionation<sup>16, 20, 21</sup> as shown in Fig. 4e.  
16  
17  
18 352 Sample loading has a significant contribution to the measured internal precision of  $\delta^{44}\text{Ca}$   
19  
20  
21 353 regardless of cup configuration and ratio combination. However, the best internal precision  
22  
23  
24 354 can be obtained using the predicted optimum condition ( $C_1$ ) in nearly all data points. By  
25  
26 355 removing the data points due to poor sample loading, measured internal precision of  $\delta^{44}\text{Ca}$   
27  
28  
29 356 under different ratio combinations of  $^{42}\text{Ca}$ - $^{48}\text{Ca}$  double spike measurements are in good  
30  
31  
32 357 agreement with the predicted internal precision, confirming the accuracy of the proposed  
33  
34  
35 358 Monte Carlo simulation method accounting for errors from Johnson noise and counting  
36  
37 359 statistics. Therefore, high precision measurements can only be obtained by rigorous sample  
38  
39  
40 360 loading protocol as well as selecting optimum ratio combination and double spike pair.  
41  
42  
43 361 Poor data points with the erratic fractionation trends (with a feature of internal precision  
44  
45 362  $>0.03\text{‰}$ ) can be easily identified during off-line data reduction process and be rejected.  
46  
47  
48 363 The fluctuations of observed internal precision around the predicted lines indicate the slight  
49  
50  
51 364 deviation of intensity of  $^{40}\text{Ca}$  from 9 V during data acquisition.

52  
53 365 The long-term reproducibility of  $\delta^{44}\text{Ca}$  for four months measurements under  $A_1$ - $D_1$   
54  
55  
56 366 combinations were found to be 0.23‰, 0.21‰, 0.21‰, 0.23‰ ( $2\sigma_{\text{SD}}$ ,  $n = 50$ ) and 0.20‰,  
57  
58  
59 367 0.17‰, 0.17‰, 0.20‰ ( $2\sigma_{\text{SD}}$ ,  $n = 18$ ) for NIST SRM 915a and NIST SRM 915b,  
60

1  
2  
3  
4  
5  
6  
7 368 respectively. Using the optimum condition (C<sub>1</sub>) produced the best external precisions for  
8  
9  
10 369 both NIST SRM 915a and NIST SRM 915b, even though the sequence of observed external  
11  
12 370 precision deviated from the predicted order (B<sub>1</sub>>A<sub>1</sub>=D<sub>1</sub>>C<sub>1</sub>). However, the external  
13  
14  
15 371 reproducibility was found to be 9 and 10 times worse than the internal precision, indicating  
16  
17  
18 372 additional uncertainty sources (e.g., filament shape, sample loading, focusing and faraday  
19  
20  
21 373 cup poison) other than Johnson noise and counting statistics. This poor agreement between  
22  
23 374 internal and external precision was also reported in previous studies.<sup>1,20,22</sup> Recent research<sup>22</sup>  
24  
25  
26 375 suggested that filament reservoir mixing effect was responsible for this big differences  
27  
28  
29 376 between measured internal precision and external precision. The Montel Carlo simulation  
30  
31  
32 377 method cannot be used to predict the external reproducibility in this case, since these  
33  
34 378 additional uncertainty sources cannot be quantified. However, certain uncertainty can be  
35  
36  
37 379 reduced by correction. Lehn *et al.*<sup>9</sup> and Schmitt *et al.*<sup>23</sup> reported an instrumental drift  
38  
39  
40 380 occurring between sessions, resulting in a systematic offset of  $\delta^{44}\text{Ca}$ . This systematic offset  
41  
42  
43 381 in  $\delta^{44}\text{Ca}$  is caused by Faraday cup deterioration (also called cup poison) in the instrument.<sup>9</sup>  
44  
45 382 <sup>16, 23</sup> In our results, a similar instrument drift was observed in  $\delta^{44}\text{Ca}$  value evaluated by all  
46  
47  
48 383 ratio combinations (A<sub>1</sub>-D<sub>1</sub>). Take the results with use of C<sub>1</sub> combination for example, as  
49  
50  
51 384 shown in Fig. 5, a systematic offset ( $\sim +0.16\%$ ) in  $\delta^{44}\text{Ca}$  value of NIST SRM 915a was  
52  
53  
54 385 found at the end of July and accompanied by a similar shift in the results of NIST SRM  
55  
56 386 915b. For this reason, the “offset correction” proposed by Lehn *et al.*<sup>9</sup> was applied to both  
57  
58  
59 387 NIST SRM 915a and NIST SRM 915b by subtracting the same offset factor (+0.16%) from  
60

1  
2  
3  
4  
5  
6  
7 388 the draft period. After the correction, mean values of  $0.00 \pm 0.15$  ( $2 \sigma_{SD}$ ,  $n=50$ ) and  $0.71 \pm$   
8  
9  
10 389  $0.11$  ( $2 \sigma_{SD}$ ,  $n=18$ ) were obtained for  $\delta^{44}\text{Ca}$  relative to NIST SRM 915a for NIST SRM 915a  
11  
12 390 and NIST 915b, respectively, with use of  $C_1$  combination. The corrected results showed a  
13  
14  
15 391 two-fold improvement compared to that of the uncorrected data. The mean value of NIST  
16  
17 392 SRM 915b using  $C_1$  ratio combination agrees well with the published values of  $\sim 0.72\%$ ,<sup>9</sup>  
18  
19 393 <sup>24</sup> confirming the accuracy of the proposed correction method. Given that the drifts in  
20  
21 394 results were similar for all ratio combinations, the external precisions can be improved in  
22  
23 395 the same scale.  
24  
25  
26  
27

28  
29 396 Overall, the observed precisions (both internal and external) can be accurately predicted  
30  
31 397 only when all the potential uncertainty sources are considered. Here, the difference between  
32  
33 398 the observed and predicted precisions suggests that there are other uncertainty sources  
34  
35 399 besides Johnson noises and counting statistics. However, optimum measurement  
36  
37 400 conditions (cup configuration and ratio combination), predicted by counting IMVs effect  
38  
39 401 using Monte Carlo simulation technique which simulates uncertainties from Johnson  
40  
41 402 noises and counting statistics, always give most precise results for both internal and  
42  
43 403 external precisions. This may be due to the fact that optimum measurement conditions were  
44  
45 404 based on the IMVs effect, and the IMVs were measured in different peak jump lines from  
46  
47 405 the same ion beam at nearly the same time (neglect the small variation of beam intensity  
48  
49 406 between different lines). The fluctuation of ion beam during different scans between one  
50  
51 407 analysis session and another session causes the deviation of observed internal and external  
52  
53  
54  
55  
56  
57  
58  
59  
60

1  
2  
3  
4  
5  
6  
7 408 precisions from those of predicted, respectively, but it does not affect the optimum  
8  
9  
10 409 condition which is determined by IMVs effect. Clearly, whenever the IMVs occurs, the  
11  
12 410 optimum condition can be determined by using the Monte Carlo technique. However,  
13  
14  
15 411 uncertainties occurred during data collection procedure, such as unequal collector and/or  
16  
17  
18 412 gain efficiency during collection, may impact this optimum condition.

19  
20 413 According to the previous studies, Monte Carlo technique which simulates uncertainty  
21  
22  
23 414 from Johnson noises and counting statistics has been successfully applied to predict  
24  
25  
26 415 experimental precision, e.g., for  $\delta^{49}\text{Ti}$ ,<sup>25</sup>  $\delta^{56}\text{Fe}$ ,<sup>7, 8, 26</sup>  $\delta^{66}\text{Zn}$ ,<sup>8</sup> and  $\delta^{114}\text{Cd}$ ,<sup>8, 27</sup> under static  
27  
28  
29 416 collection mode using MC-ICPMS. It can thus be inferred that the proposed Monte Carlo  
30  
31  
32 417 model can be used as a powerful predetermination of optimum measurement conditions for  
33  
34  
35 418 all non-stable isotopes measured by DS-TIMS or DS-MC-ICPMS under peak jump  
36  
37  
38 419 collection mode.

39  
40 420

## 41 42 421 **Conclusions**

43  
44  
45 422 This study presents an efficient model for theoretically predicting the internal precision of  
46  
47  
48 423 double spike technique when peak jump mode is employed, using Monte Carlo simulation  
49  
50  
51 424 technique in considering uncertainty contributions from Johnson noise and counting  
52  
53  
54 425 statistics. The model was assessed by the investigation of three different double spike pairs  
55  
56  
57 426 of  $^{42}\text{Ca}$ - $^{48}\text{Ca}$ ,  $^{43}\text{Ca}$ - $^{48}\text{Ca}$ , and  $^{46}\text{Ca}$ - $^{48}\text{Ca}$  which commonly cannot be measured in static  
58  
59  
60 427 collection mode. Predicted results show 25%, 20%, and 25% improvements by using



1  
2  
3  
4  
5  
6  
7 428 optimum cup configurations and ratio combinations for  $\delta^{44}\text{Ca}$  with use of  $^{42}\text{Ca}$ - $^{48}\text{Ca}$ ,  $^{43}\text{Ca}$ -  
8  
9  
10 429  $^{48}\text{Ca}$ , and  $^{46}\text{Ca}$ - $^{48}\text{Ca}$  double spike, respectively. Observed results from repeat measurements  
11  
12 430 of NIST SRM 915a and NIST SRM 915b confirm the feasibility of the proposed model for  
13  
14  
15 431 predicting optimal cup configuration and ratio combination. Long-term reproducibility can  
16  
17  
18 432 be further improved if a rigorous analysis condition protocol is available since extra error  
19  
20  
21 433 source has a significant impact to the external precision of  $\delta^{44}\text{Ca}$ .

22  
23 434 As demonstrated for Ca isotope measurements, Monte Carlo simulation is a useful tool  
24  
25  
26 435 in achieving accurate and precise results because of the following reasons: 1) optimal  
27  
28  
29 436 double spike predicted by using static collection mode is also suitable for peak jump  
30  
31  
32 437 collection mode; 2) it provides a clear and simple selection of cup configuration in each  
33  
34  
35 438 line when peak jump mode is used; 3) measurement precision can be improved by using  
36  
37  
38 439 optimal ratio combination during data reduction when all IMVs are obtained; 4) difference  
39  
40  
41 440 in ion count per sample caused by difference in isotope abundances can be reduced by  
42  
43  
44 441 using appropriate integration times in different lines, while maintaining good measurement  
45  
46  
47 442 precision. The proposed method is expected to be applicable to other isotopes which cannot  
48  
49  
50 443 be measured simultaneously in a single line using double spike technique.

51 444

#### 52 53 445 **Acknowledgements**

54  
55  
56 446 We thank Tom Owens from Center for Isotope Geochemistry, University of California,  
57  
58  
59 447 Berkeley for his invaluable help in laboratory work. This study has been financially  
60

1  
2  
3  
4  
5  
6  
7 448 supported by the National Natural Science Foundation of China (41273005 and 41473007),  
8  
9  
10 449 the Ministry of Education of China (IRT0441 and B07039), a special fund from the State  
11  
12 450 Key Laboratory of Geological Processes and Mineral Resources (GPMR201106 and  
13  
14  
15 451 MSFGPMR01) and the Fundamental Research Funds for the Central Universities.  
16  
17  
18  
19  
20  
21  
22  
23  
24  
25  
26  
27  
28  
29  
30  
31  
32  
33  
34  
35  
36  
37  
38  
39  
40  
41  
42  
43  
44  
45  
46  
47  
48  
49  
50  
51  
52  
53  
54  
55  
56  
57  
58  
59  
60

453 **References**

- 454 1 Donald J. DePaolo, *Rev. Mineral. Geochem.*, 2004, **55**, 255-288.
- 455 2 M. S. Fantle and E. T. Tipper, *Earth-Science Reviews.*, 2013 **129**, 148-177.
- 456 3 Goldberg, T., et al. *J. Anal. At. Spectrom.*, 2013, **28**, 724-735.
- 457 4 M. H. Dodson, *Journal of Physics E: Scientific Instruments*, 1969, **2**, 490.
- 458 5 M. H. Dodson, *Journal of Scientific Instruments*, 1963, **40**, 289.
- 459 6 L. Yang, *Mass Spectrom Reviews.*, 2009, **28**, 990-1011.
- 460 7 J. F. Rudge, B. C. Reynolds and B. Bourdon, *Chem. Geol.*, 2009, **265**, 420-431.
- 461 8 S. G. John, *J. Anal. At. Spectrom.*, 2012, **27**, 2123-2131
- 462 9 G. O. Lehn, A. D. Jacobson and C. Holmden, *Int. J. Mass Spectrom.*, 2013, **351**, 69-  
463 75.
- 464 10 A. Heuser, A. Eisenhauer, N. Gussone, B. Bock, B. T. Hansen and T. F. Nägler, *Int. J.*  
465 *Mass Spectrom.*, 2002, **220**, 385-397.
- 466 11 J. Skulan, D. J. DePaolo and T. L. Owens, *Geochim. Cosmochim. Acta*, 1997, **61**, 2505-  
467 2510.
- 468 12 S. Huang, J. Farkaš and S. B. Jacobsen, *Earth Planet. Sci. Lett.*, 2010, **292**, 337-344.
- 469 13 S. Ripperger and M. Rehkämper, *Geochim. Cosmochim. Acta*, 2007, **71**, 631-642.
- 470 14 T. M. Johnson, M. J. Herbel, T. D. Bullen and P. T. Zawislanski, *Geochim. Cosmochim.*  
471 *Acta*, 1999, **63**, 2775-2783.
- 472 15 W. A. Russell and D. A. Papanastassiou and T. A. Tombrello, *Geochim. Cosmochim.*  
473 *Acta*, 1978, **42**, 1075-1090.
- 474 16 C. Holmden and N. Bélanger, *Geochim. Cosmochim. Acta*, 2010, **74**, 995-1015.
- 475 17 S. F. Boulyga, *Mass Spectrom Reviews.*, 2010, **29**, 685-716.
- 476 18 J. I. Simon and D. J. DePaolo, *Earth Planet. Sci. Lett.*, 2010, **289**, 457-466.
- 477 19 F. Wombacher, A. Eisenhauer, A. Heuser and S. Weyer, *J. Anal. At. Spectrom.*, 2009,  
478 **24**, 627-636.
- 479 20 M. Fantle and T. Bullen, *Chem. Geol.*, 2009, **258**, 50-64.
- 480 21 Hart S. R. and Zindler A, *Int. J. Mass Spectrom. Ion Proc.*, 1989, **89**, 287-301.
- 481 22 G. O. Lehn and A. D. Jacobson, *J. Anal. At. Spectrom.*, 2015, **30**, 1571-1581.
- 482 23 A.-D. Schmitt, S. J. G. Galer and W. Abouchami, *J. Anal. At. Spectrom.*, 2009, **24**,  
483 1079-1088.
- 484 24 A. Heuser and A. Eisenhauer, *Geostand. Geoanal. Res.*, 2008, **32**, 311-315.
- 485 25 M.-A. Millet and N. Dauphas, *J. Anal. At. Spectrom.*, 2014, **29**, 1444-1458.
- 486 26 M.-A. Millet, J. A. Baker and C. E. Payne, *Chem Geol.*, 2012, **304**, 18-25.
- 487 27 Z. Xue, M. Rehkämper, M. Schönbächler, P. Statham and B. Coles, *Anal bioanal*  
488 *chem.*, 2012, **402**, 883-893.

489

490

491 **Table 1.** Isotopic abundance (%) of spikes and reference material.

Material	<sup>40</sup> Ca	<sup>42</sup> Ca	<sup>44</sup> Ca	<sup>48</sup> Ca
<sup>42</sup> Ca single spike	0.004	94.49	0.04	0.02
<sup>48</sup> Ca single spike	0.001	0.01	0.001	97.80
<sup>42</sup> Ca- <sup>48</sup> Ca double spike <sup>a</sup>	4.04	41.90	0.43	53.43
NIST SRM 915a <sup>b</sup>	98.89	0.64	2.06	0.18

<sup>a</sup> Calibrated composition. <sup>b</sup> Taken from Russell *et al.*<sup>15</sup>

492

493 **Table 2.** TIMS operating conditions

Instrument parameter	Setting
Cup configuration	Line 1: $^{39}\text{K}$ (L3), $^{40}\text{Ca}$ (L2), $^{42}\text{Ca}$ (C), $^{43}\text{Ca}$ (H1), $^{44}\text{Ca}$ (H2) Line 2: $^{42}\text{Ca}$ (L3), $^{44}\text{Ca}$ (L1), 45.50 (C), $^{48}\text{Ca}$ (H3)
Resistors	$10^{11}\Omega$ for all amplifiers
Intensity	$^{40}\text{Ca}$ about 9 V within 10% variation
Integration time	8 s in each line
Idle time	4 s after each line
Blocks number	5
Cycles number	20
Baseline	before each block
Focus	warm-up and every 2 blocks
peak center	warm-up and every 2 blocks
Amplifier rotation	After each block
Sample heating program	Setting
Step 1: ION filament <sup>a</sup>	1000 mA/min to 1420 °C
Step 2: EVPA filament <sup>b</sup>	250 mA/min to 1500 mA
Step 3: EVPA filament	60 mA/min to 1650 mA
Step 4: EVPA filament	Waite for 5 min, focus
Step 5: EVPA filament	Open valve, 60 mA/min to 4000 mV (pilot mass $^{40}\text{Ca}$ )
Step 6: EVPA filament	30 mA/min to 7000 mV (pilot mass $^{40}\text{Ca}$ ), focus
Step 7: EVPA filament	10 mA/min to 9000 mV (pilot mass $^{40}\text{Ca}$ ), focus
Step 8: Start data evaluation	
<sup>a</sup> ION filament = ionization filament. <sup>b</sup> EVAP filament = evaporation filament	

494

1  
2  
3  
4  
5  
6  
7 **Figure captions**  
8

9  
10 **Fig. 1** Schematic diagram of theoretically possible cup configurations for Ca isotope ratio  
11  
12 measurements with use of  $^{42}\text{Ca}$ - $^{48}\text{Ca}$ ,  $^{43}\text{Ca}$ - $^{48}\text{Ca}$ ,  $^{46}\text{Ca}$ - $^{48}\text{Ca}$  double spikes. Configuration (a)  
13  
14 and (b) measure  $^{42}\text{Ca}$  or  $^{43}\text{Ca}$  or  $^{46}\text{Ca}$  in both lines, but measure  $^{44}\text{Ca}$  in a different line.  
15  
16 Configuration (c) and (d) measure  $^{44}\text{Ca}$  in both lines, but measure  $^{42}\text{Ca}$  or  $^{43}\text{Ca}$  or  $^{46}\text{Ca}$  in a  
17  
18 different line. Configuration (e) measures all isotopes in one line. Dashed cups represent  
19  
20 the case with use of  $^{43}\text{Ca}$ - $^{48}\text{Ca}$ , and  $^{46}\text{Ca}$ - $^{48}\text{Ca}$  double spike, respectively.  
21  
22  
23  
24  
25  
26  
27

28  
29 **Fig. 2** Monte Carlo estimation of the internal precision ( $2\sigma_{\text{SEM}}$ ) of  $\delta^{44}\text{Ca}$  arising from  
30  
31 various double spike pairs, proportion of primary spike in double spike and proportion of  
32  
33 double spike in mixture and use of different ratio combinations. Each ratio combination is  
34  
35 corresponding to one cup configuration presented in Fig. 1. A<sub>1</sub>-A<sub>3</sub>:  $^{40}\text{Ca}_{\#1}/^{4i}\text{Ca}_{\#1}$ ,  
36  
37  $^{44}\text{Ca}_{\#1}/^{4i}\text{Ca}_{\#1}$ ,  $^{48}\text{Ca}_{\#2}/^{4i}\text{Ca}_{\#2}$  ( $i = 2, 3$  or  $6$ ). B<sub>1</sub>-B<sub>3</sub>:  $^{40}\text{Ca}_{\#1}/^{4i}\text{Ca}_{\#1}$ ,  $^{44}\text{Ca}_{\#2}/^{4i}\text{Ca}_{\#2}$ ,  $^{48}\text{Ca}_{\#2}/^{4i}\text{Ca}_{\#2}$ .  
38  
39 C<sub>1</sub>-C<sub>3</sub>:  $^{40}\text{Ca}_{\#1}/^{44}\text{Ca}_{\#1}$ ,  $^{4i}\text{Ca}_{\#1}/^{44}\text{Ca}_{\#1}$ ,  $^{48}\text{Ca}_{\#2}/^{44}\text{Ca}_{\#2}$ . D<sub>1</sub>-D<sub>3</sub>:  $^{40}\text{Ca}_{\#1}/^{44}\text{Ca}_{\#1}$ ,  $^{4i}\text{Ca}_{\#2}/^{44}\text{Ca}_{\#2}$ ,  
40  
41  $^{48}\text{Ca}_{\#2}/^{44}\text{Ca}_{\#2}$ . E<sub>1</sub>-E<sub>3</sub>:  $^{40}\text{Ca}_{\#1}/^{44}\text{Ca}_{\#1}$ ,  $^{4i}\text{Ca}_{\#1}/^{44}\text{Ca}_{\#1}$ ,  $^{48}\text{Ca}_{\#1}/^{44}\text{Ca}_{\#1}$ . The subscript numbers  
42  
43  
44  
45  
46  
47  
48 (e.g., A<sub>1</sub>) denote the double spike pairs: 1 =  $^{42}\text{Ca}$ - $^{48}\text{Ca}$ ; 2 =  $^{43}\text{Ca}$ - $^{48}\text{Ca}$ ; 3 =  $^{46}\text{Ca}$ - $^{48}\text{Ca}$ . The  
49  
50 total intensity and individual integration time for each line used for Monte Carlo estimation  
51  
52 were 10 V and 8 s, respectively. The abundances of primary spikes used in the calculation  
53  
54 were all assumed to be 100% enriched. Only predicted internal precision within 0.060‰ is  
55  
56  
57  
58  
59  
60

1  
2  
3  
4  
5  
6  
7 514 shown in the contour plots. The filled circle marks the optimal  $^{42}\text{Ca}$ - $^{48}\text{Ca}$  double spike  
8  
9 515 composition tested in this study ( $q=^{42}\text{Ca}/(^{42}\text{Ca}+^{48}\text{Ca})=0.44$ ,  $p=\text{double spike}/\text{mixture}=0.12$ )  
10  
11 516

12  
13 **Fig. 3** The effect of integration time on predicted internal precision ( $2\sigma_{\text{SEM}}$ ) of  $\delta^{44}\text{Ca}$  under  
14  
15 different cup configurations and ratio combinations. Internal precision is predicted by  
16  
17 Monte Carlo simulation with total intensity of 10V and use of an optimum  $^{42}\text{Ca}$ - $^{48}\text{Ca}$  double  
18  
19 519 spike. Integration time in line one ( $\Delta t_1$ ) and line two ( $\Delta t_2$ ) are allowed to vary independently,  
20  
21 520 while keeping a constant total integration time ( $\Delta t$ ) of 16s (a). Total integration time varies  
22  
23 521 from 2s to 16s, while integration time in line one and line two are set equal (b).  
24  
25 522  
26  
27 523

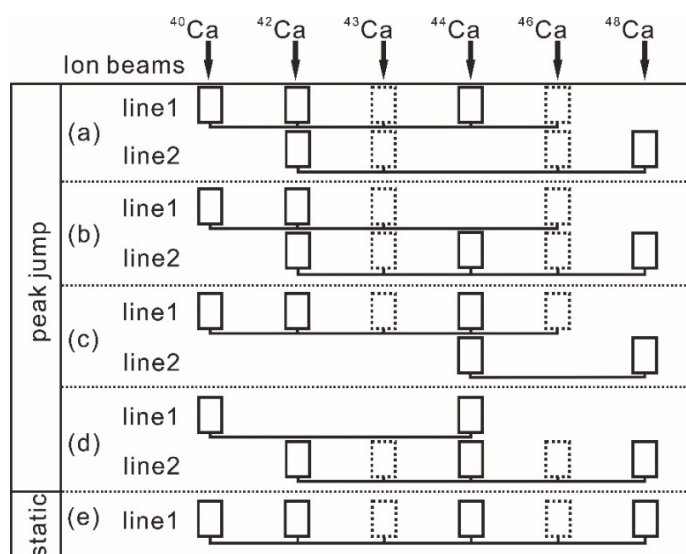
28  
29  
30  
31 **Fig. 4** Comparison of observed and predicted internal precision of  $\delta^{44}\text{Ca}$  under different  
32  
33 ratio combinations. Data points are composed by 61 measurement results of NIST SRM  
34  
35 525 915a (white area) and 21 measurement results of NIST SRM 915b (grey area). Observed  
36  
37 526 values calculated by using ratio combination  $^{40}\text{Ca}_{\#1}/^{42}\text{Ca}_{\#1}$ ,  $^{44}\text{Ca}_{\#1}/^{42}\text{Ca}_{\#1}$ ,  $^{48}\text{Ca}_{\#2}/^{42}\text{Ca}_{\#2}$  (a);  
38  
39 527  
40  
41 528  $^{40}\text{Ca}_{\#1}/^{42}\text{Ca}_{\#1}$ ,  $^{44}\text{Ca}_{\#2}/^{42}\text{Ca}_{\#2}$ ,  $^{48}\text{Ca}_{\#2}/^{42}\text{Ca}_{\#2}$  (b);  $^{40}\text{Ca}_{\#1}/^{44}\text{Ca}_{\#1}$ ,  $^{42}\text{Ca}_{\#1}/^{44}\text{Ca}_{\#1}$ ,  $^{48}\text{Ca}_{\#2}/^{44}\text{Ca}_{\#2}$  (c);  
42  
43 529 and  $^{40}\text{Ca}_{\#1}/^{44}\text{Ca}_{\#1}$ ,  $^{42}\text{Ca}_{\#2}/^{44}\text{Ca}_{\#2}$ ,  $^{48}\text{Ca}_{\#2}/^{44}\text{Ca}_{\#2}$  (d). The open symbols represent samples that  
44  
45  
46  
47 530 had an erratic pattern of fractionation trend during the TIMS measurements. Inserted  
48  
49 531 figures (e) and (f) depict typical fractionation trends (presented by variation of  $^{42}\text{Ca}/^{48}\text{Ca}$   
50  
51 532 ratio during 100 scans) of bad and good sample-loading results, respectively. Solid lines  
52  
53 533 indicate the predicted internal precision, while dash lines represent the mean value of all  
54  
55  
56  
57 534 the observed internal precision.  
58  
59  
60

1  
2  
3  
4  
5  
6  
7 535

8  
9  
10 536 **Fig. 5** Four month measurements of  $\delta^{44}\text{Ca}$  in NIST SRM 915a and SRM 915b. Data points  
11  
12 537 which show an erratic pattern of fractionation trend were rejected during off-line data  
13  
14  
15 538 reduction. In (a) data points are presented without offset correction, while in (b) have been  
16  
17  
18 539 applied with offset correction. The red line is the reference values  $0.72\text{‰}^{9, 24}$  of  $\delta^{44}\text{Ca}$  in  
19  
20  
21 540 NIST SRM 915b. Error bars are  $2\sigma_{\text{SEM}}$ .

22  
23 541  
24  
25  
26  
27  
28  
29  
30  
31  
32  
33  
34  
35  
36  
37  
38  
39  
40  
41  
42  
43  
44  
45  
46  
47  
48  
49  
50  
51  
52  
53  
54  
55  
56  
57  
58  
59  
60



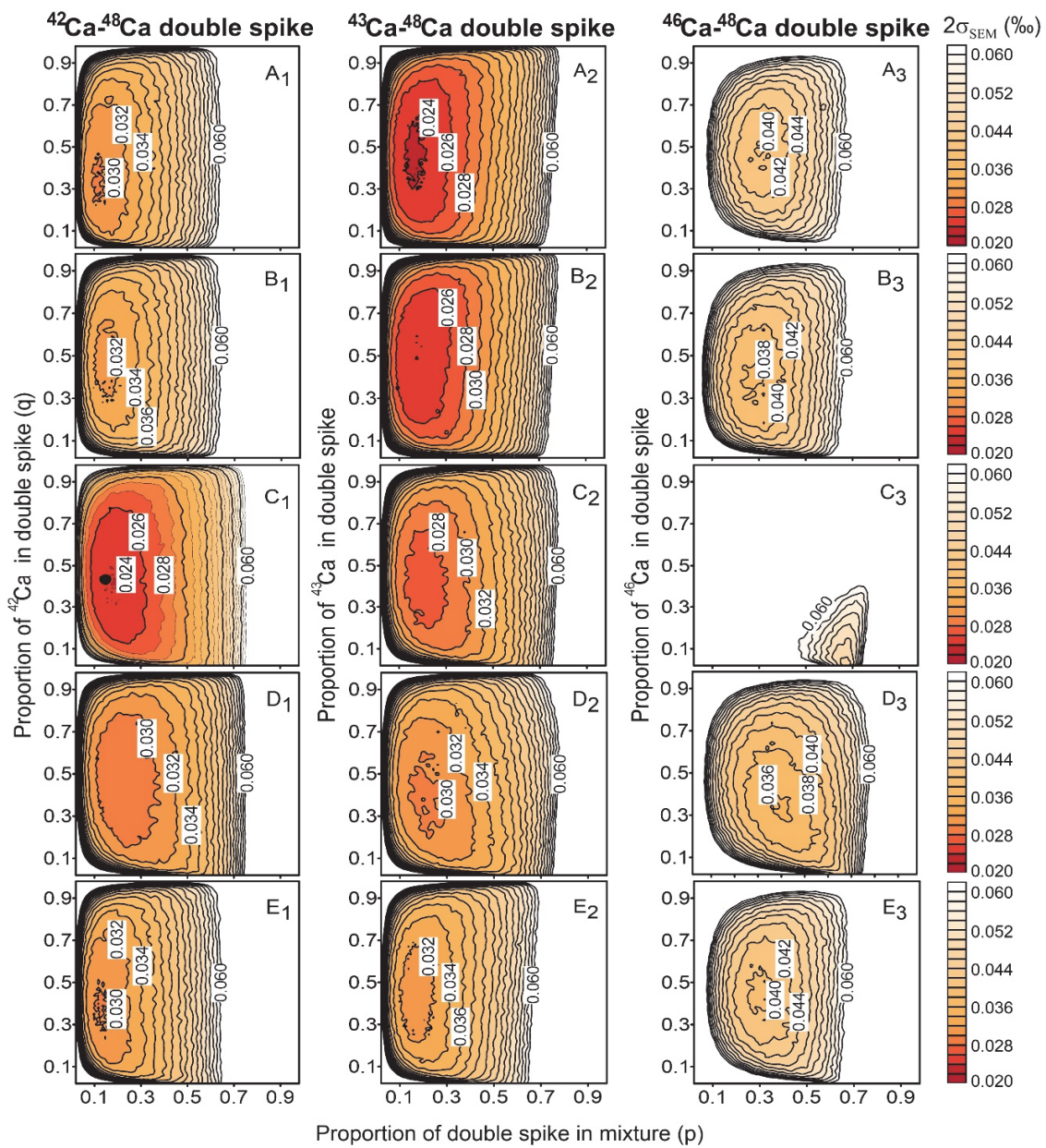
542 **Figure 1**

543

544

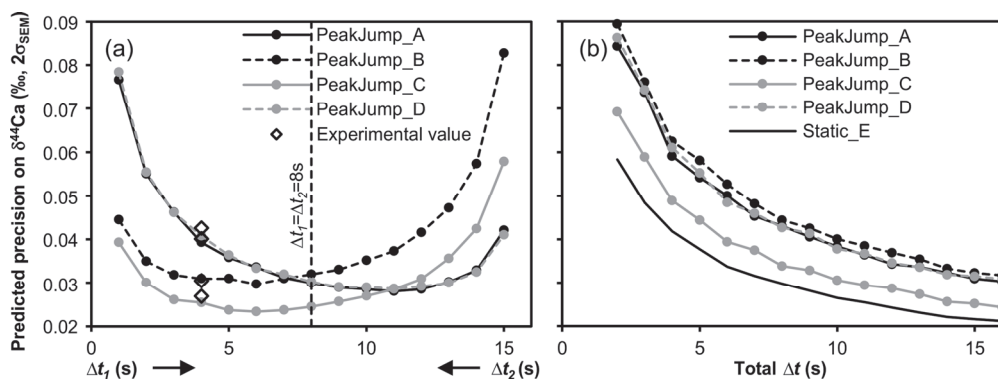
545 Figure 2

546



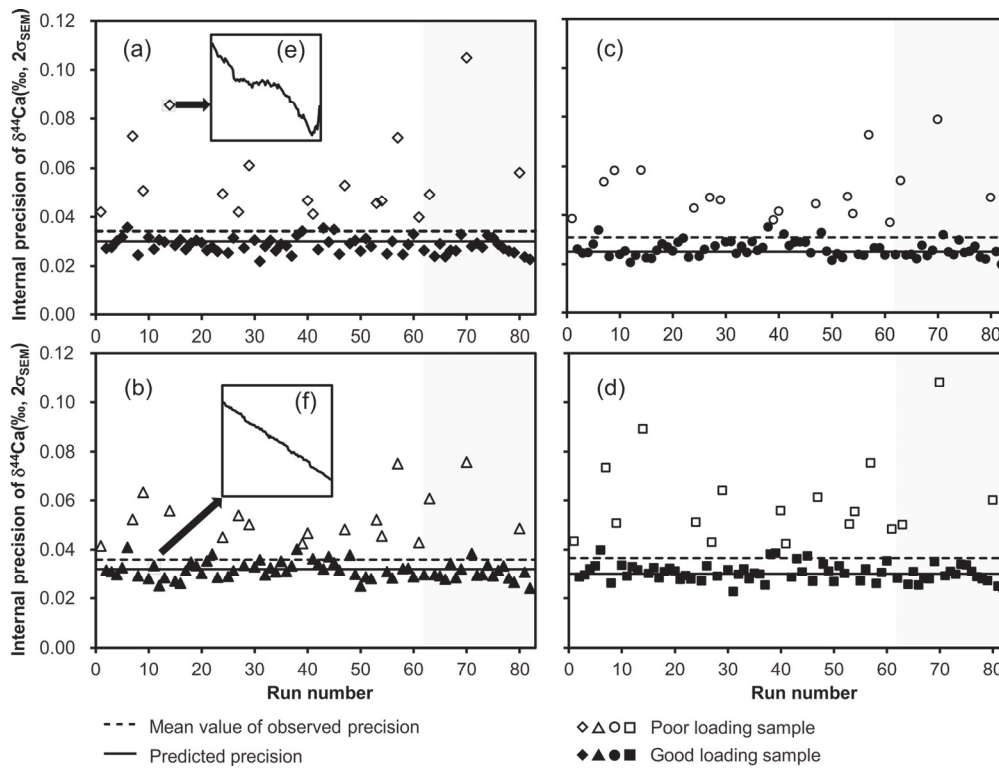
547

548

549 **Figure 3**

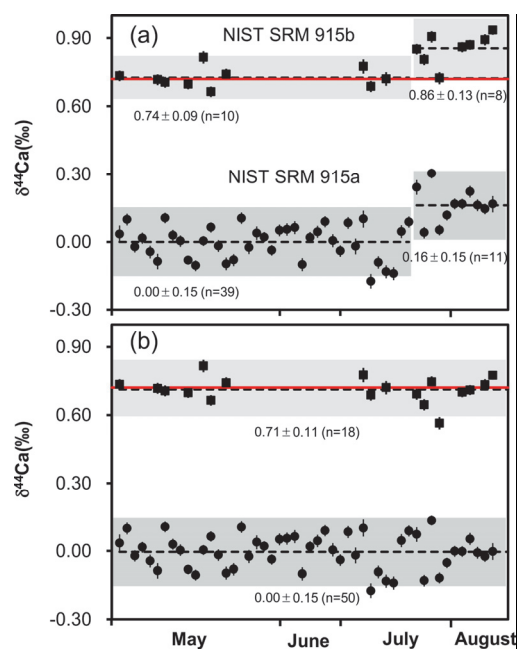
550

551

552 **Figure 4**

553

554

555 **Figure 5**

556

557

558